Pak. J. Bot., 58(4) April, 2026.

ARTICLE | DOI: http://dx.doi.org/10.30848/PJB2026-4(7)

BIOCHEMICAL ASSESSMENT AND THERAPEUTIC PROFILING OF *ROSMARINUS OFFICINALIS* LEAF EXTRACT-MEDIATED GOLD NANOPARTICLES

AJMAL M. THEYYATHEL[1], ANIMA NANDA[2*], MOHMMAD ASHAQ SOFI[3] AND B.K. NAYAK[4]

[1, 2&3]Department of Biomedical Engineering, Sathyabama Institute of Science and Technology, Chennai- 600119, India
[4]Department of Botany, K. M. Govt. Institute for Postgraduate Studies and Research (Autonomous), Puducherry-605008, India

*Corresponding author's email: animananda72@gmail.com

Abstract

Green chemistry offers sustainable approaches to nanoparticle synthesis by avoiding toxic reagents and utilizing plant-derived bioactive compounds. *Rosmarinus officinalis* leaves, rich in flavonoids, tannins, alkaloids, and phenolics, were employed to synthesize gold nanoparticles (RO-AuNPs) within 10 minutes at room temperature. The nanoparticles were characterized by UV–Vis, FESEM, XRD, and EDX analyses. RO-AuNPs were predominantly spherical, monodisperse, and measured 16–57 nm in size. EDX confirmed gold as the major element, while XRD revealed a face-centred cubic structure. RO-AuNPs displayed antimicrobial activity against *Enterococcus faecalis*, *Escherichia coli*, *Staphylococcus aureus*, *Pseudomonas aeruginosa*, and *Candida albicans*, with MIC values of 128, 64, 128, 64, and 256 µg/mL, respectively. The crude extract showed no such activity. Cytotoxicity assays on A549 lung cancer cells yielded IC_{50} values of 33.60 and 23.12 µg/mL at 24 and 48 h, respectively. Apoptotic induction was confirmed by AO/PI staining and upregulation of Cytochrome C, indicating activation of the intrinsic mitochondrial apoptotic pathway. Additionally, significant downregulation of IL-6 expression suggested anti-inflammatory activity with potential implications for tumor microenvironment modulation. Collectively, these findings demonstrate that *R. officinalis*-mediated gold nanoparticles possess multifunctional bioactivities and represent a promising, eco-friendly platform for future antimicrobial and anticancer applications.

Key words: *Rosmarinus officinalis*, green synthesis, gold nanoparticles, antimicrobial activity, cytotoxicity, apoptosis, anti-inflammatory, *Cytochrome C*, *IL-6*

Introduction

Nanotechnology has been extensively studied and applied in various scientific sectors, including physical, agricultural, chemical, and biomedical (Shang*et al*., 2019; Ma *et al*., 2024;Sharma*et al*., 2021; Gong*et al*., 2021). Since nanotechnology has been around for a while, many different kinds of nanostructures have been created and are now used in a variety of fields and industries. Metal and metal oxide nanoparticles, carbon-based nanomaterials, silicon-based nanomaterials, ceramic nanoparticles, and polymeric nanoparticles are a few examples of nanomaterials. These materials have found applications in diverse fields such as medicine, electronics, photonics, food science, cosmetics, agriculture, textiles, and space technologies (Schaming & Remita, 2015; Sajid, 2022; Yaqoob *et al*., 2020; Kamyshny&Magdassi, 2019; Levchenko*et al*., 2018).

To date, various synthetic approaches have been employed by researchers to synthesize nanomaterials, encompassing chemical, physical and biological methods. The physical and chemical methods are environmentally or biologically incompatible, economically unsound, and inefficient in production. Compared to the physical or chemical methods, a green synthetic approach has been widely accepted for synthesizing nanomaterials on a large scale. This method utilizes plants, plant products, or extracts for synthesizing nanomaterials. Green mediated synthetic approach is relatively eco-friendly, less time-consuming, highly productive, and economically justified (Sofi *et al*., 2022).

A great diversity of metal nanomaterials have been synthesized and explored. Among these, noble metals have also been widely and significantly explored for biomedical applications owing to their inert and biocompatible nature (Choi*et al*., 2021; Azharuddin *et al*., 2019).Gold nanomaterials are considered highly biocompatible due to their unique features, including excellent optoelectronic properties, high surface-to-volume ratio, diverse morphologies, and chemical inertness. These attributes make them widely applicable in various biomedical fields. They are being employed in biosensing, different imaging technologies (X-ray, Thermo/photoacoustic, microscopic optical imaging), antimicrobial agents, anticancer applications, biosensors, biomedical device coatings, gene manipulation and delivery, drug delivery, treatment and diagnostics of various diseases, and the development of gold stains (Singh *et al*., 2018; Siddique& Chow, 2020); Botteon *et al*., 2021).

Hence their formation and consumption have increased many folds over the last few decades, though their uses date back to ancient times. So far, ample literature is available about the synthesis of gold nanomaterials from extracts of plants incluing *Capsicum annum, Populus alba* and *Acorus calamus* (Patil et al., 2023; Guliani et al., 2021; Peng, et al., 2024). Plants, being complicated bio machines, have a diversity of natural phytochemicals, which include flavonoids, terpenoids, anthocyanins, carotenoids, alkaloids, phenolic acids, proteins, vitamins, hormones, and other biomolecules which have efficient capabilities of

Received: 04-09-2026 | Revised: 18-11-2025 | Accepted: 02-12-2025 | Online: 05-01-2026

reducing gold ions to form metal nanoaggregates and their subsequent. This spares the need to add conventional harmful chemicals as stabilizers or surfactants (Hassanisaadi*et al*., 2021; Castillo-Henríquez *et al*., 2020). Gold nanoparticles synthesized using phytochemicals have demonstrated the ability to damage microbial cell membranes, induce oxidative stress in cancer cells, and modulate inflammatory signaling pathways. These effects are often enhanced by the bioactive molecules from the plant extracts used in synthesis (Bharadwaj *et al*., 2021; Morsy*et al*., 2025).

Rosmarinus officinalis, belonging to the *Lamiaceae* family, originates from Europe, Africa, and Central Asia, but is now grown globally because of its wide range of applications (Sofi*et al*., 2022). Its aromatic leaves are widely used to enhance the flavor of food and beverages, and are also brewed in herbal teas (Salamatullah *et al*., 2021). Traditionally, *R. officinalis* has been used in combination with other medicinal plants to treat a variety of ailments, enhancing the efficacy of therapeutic regimens (Rahbardar & Hosseinzadeh (2020).Some of the reported medicinal uses of *R. officinalis*, alone or in combination with other medicinal formulations, include the treatment of nervous system-related disorders (such as insomnia, anxiety, depression, impaired cognition, and Alzheimer's disease), gastrointestinal disorders (such as acid reflux, stomach pain, dyspepsia, nausea, vomiting, flatulence, and infant colics), headaches, migraine, hair loss, antihyperlipidemic, antihyperglycemic, bronchitis, and wound healing. Additionally, *R. officinalis* is recognized for its wide-ranging bioactivities, including anticancer, antiviral, antimicrobial, anti-inflammatory, and antioxidant properties, especially when processed through various solvent extractions or formulated into nanocomposites (Theyyathel *et al*., 2025; Halahlah *et al*., 2021).

Although numerous studies have reported plant-mediated synthesis of gold nanoparticles, limited investigations have focused on *R. officinalis*-derived gold nanoparticles with combined antimicrobial and anticancer evaluation supported by mechanistic insights. While *R. officinalis* is known for its antioxidant, anti-inflammatory, and anticancer properties, the enhancement of these bioactivities through nanoparticle fabrication remains insufficiently explored. The present study addresses this gap by synthesizing gold nanoparticles using *R. officinalis* leaf extract and evaluating their antimicrobial efficacy, cytotoxic potential against lung cancer cells, and underlying molecular mechanisms involving apoptosis and inflammatory modulation.

Materials and Methods

Chemicals: The FBS, along with the antibiotic–antimycotic solution, was supplied by Sigma Aldrich (USA.), while DMEM and MTT were obtained from Gibco (USA).) and SRL Chemicals (India), respectively. 96 well plate, laboratory culture wares and disposables were purchased from Tarsons (India).

Collection and processing of plant material: The *Rosmarinus officinalis* leaves (Fig. 1(a, b) were collected from Daksum Anantnag Kashmir, India (alt. 2425 meters approx. above sea level). The plant specimen was taxonomically identified and deposited at University of Kashmir herbarium. The fresh leaves were washed well under running water to get rid of any dirt on the surface. They were then left to dry in the shade for ten days under hygienic conditions to prevent the growth of mold or other contaminants. The dried leaves were finely powdered with the aid of an electrical grinder.

Preparation of leaf extract: 10 grams of finely ground powder was combined with 100 mL deionized water in a flask. The mixture was stirred slowly while being boiled for 10 minutes. The extracts were obtained by filtering the mixture via Whatman No.1 filter paper and were refrigerated until used.

Synthesis of *Rosmarinus officinalis* gold nanoparticles: RO- AuNPs (*Rosmarinus officinalis* gold nanoparticles) were synthesized by adding 3mL plant extract to 97 mL of 1 mM auric chloride (purchased from Loba cheme Pvt. Ltd., Mumbai) in a flask at room temperature, and after 10 minutes of gentle stirring, the color of the mixture turned to ruby red as shown in Fig.2.

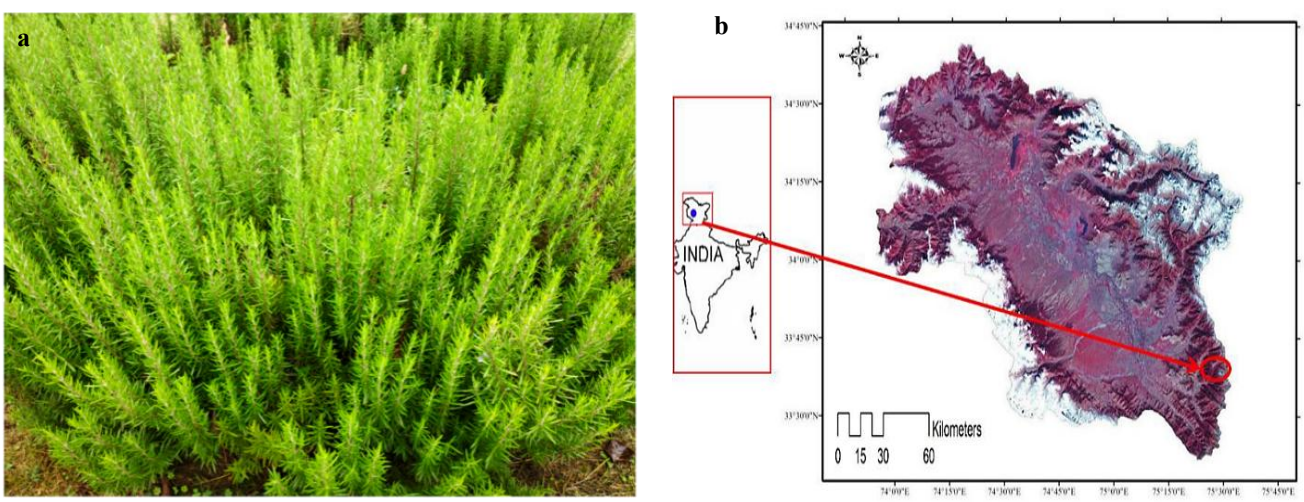

Fig. 1. **(a)** *Rosmarinus officinalis* Plant; **(b)** illustrates the collection site at Daksum Kokernag, Kashmir, India, (75°26′6″ E, 33°36′43″ N ; alt. ~2425 m). Voucher specimen: **2833-(KASH)**.

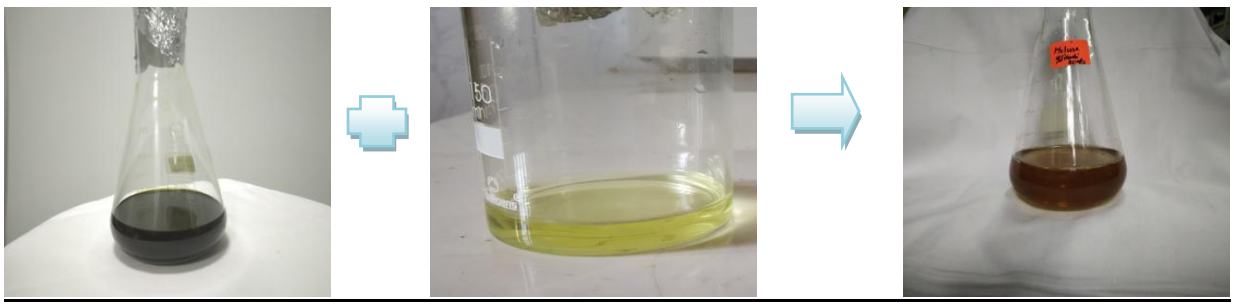

Fig. 2. Schematic representation of the formation of ruby-red colored *R. officinalis* gold nanoparticles.

Characterization: The nanoparticles were characterized by employing the usual characterization techniques like UV-visible spectroscopy, X-ray diffraction, FESEM, and EDX. A UV-Vis spectroscopic analysis was performed by using a spectrophotometer at a lambda ranging from 300–700 nm. The sample was subjected to X-ray diffraction (XRD) analysis using X8 Kappa APEX II (Bruker) diffractometer. Further analytical information about particle size range and morphology was retrieved from FESEM (Hitachi S4800) and percentage elemental composition from energy dispersive X-ray (EDX) imaging.

Antimicrobial Assay: The antimicrobial activity was evaluated against five pathogens: *E. faecalis* ATCC 29212 and *S. aureus* ATCC 25923(Gram-positive), *P. aeruginosa* ATCC 15442 and *E. coli ATCC* 11229(Gram-negative), and *C. albicans ATCC* 10231 (fungus. The test pathogens (10^4–10^6 CFU/mL) were swabbed by using cotton swabs onto the Mueller Hinton Agar medium to obtain the uniform growth of microbial cells. The agar medium in Petri plates was perforated with 6 mm diameter holes using a cork borer. Thereafter, the wells were filled with varying micro volumes (25, 50, 75, and 100 uL) of RO-AuNPs taken from freshly prepared 1 mg/mL stock solution. Ampilox (for gram-positive), Ciprofloxacin (gram-negative), and Fluconazole (fungus) were used as positive controls in the experiment. The negative control used in the experiment was DMSO. After 24 h of incubation at 37ºC, measurement of zones of inhibition was done. The MIC of RO-AuNPs against selected pathogens was calculated by using the broth dilution technique (Sofi *et al*., 2022; Gabrielson *et al*., 2002).

Cytotoxic assay: A549 cells acquired from NCCS (Pune, India) were maintained in DMEM supplemented with 10% FBS) at 37°C in a humidified 5% CO_2. For cytotoxicity evaluation, approximately 6,000 cells per well were seeded into 96-well plates and incubated for 24 hs to enable cell attachment. The culture medium was substituted with DMEM enriched with 3% FBS, and cells were then subjected to varying concentrations of RO-AuNPs (10–60 µg/mL) for durations of 24 and 48 h. Later on,10µl of MTT dye from the stock solution of (5mg/mL) was supplemented into each well and then again incubated for 4 h at 37ºC.The cells treated with no extract were set as control. After the experiment, the media and MTT reagent were removed, and 100µL of DMSO was added to each well and were gently shaken. Finally, OD was measured at 590 nm to assess the cytotoxic impact compared to untreated control (Sofi *et al*., 2025).

Cell viability % = (Absorbance of treated cells / Absorbance of control cells) x 100

AO/PI Dual staining: To detect apoptotic and necrotic changes, A549 cancer cells were incubated with RO-AuNPs for 24 h, followed by PBS washing. Cells were then stained with equal volumes (5 µL each) of AO and PI solutions (100 µg/mL). AO penetrates all cells and fluoresces green in live cells, while PI enters only compromised membranes, binding to DNA and fluorescing red. This technique distinguishes between viable, apoptotic, and necrotic cells under a fluorescence microscope (Jaisankar*et al*., 2022).

Isolation of Total RNA: RNA extraction was performed under strict RNase-free conditions using Tri Reagent (GeNei, India), adapting the Chomczynski &Sacchi, 1987)protocol. Initial cell lysis was followed by a 5-minute incubation to ensure nucleoprotein complex dissociation. For phase separation, 200 µL chloroform was vigorously mixed into the lysate, followed by centrifugation (12,000 rcf, 15 minutes, 4°C). The clear upper aqueous phase, containing RNA, was carefully aspirated to avoid interphase contamination. The RNA-containing aqueous phase was carefully aspirated to avoid interphase contamination. RNA precipitation was performed by adding 250 µL isopropanol, followed by incubation for 15 minutes and centrifugation at 12,000 rcf for 15 minutes at 4°C. Afterward, the pellet underwent two washes with 75% ethanol, was left to air-dry completely, and was then dissolved in 40 µL of DEPC-treated water. Incubation at 55°C for 20 minutes ensured complete RNA dissolution. Post-incubation, the RNA solution was briefly placed on ice to cool and was stored at –80°C.

Synthesis of cDNA and real-time PCR: Synthesis of complementary DNA (cDNA) was performed using 0.5–1.0 µg of RNA and the GeNei cDNA Conversion Kit. The RNA was primed with random hexamers and incubated at 72°C for 10 minutes, then immediately cooled on ice. Reverse transcription was conducted using M-MLV reverse transcriptase in the presence of dNTPs and RT buffer in a 50 µL reaction volume. The resulting cDNA was then used for quantitative PCR using SYBR Green dye for gene expression analysis. The following primer sequences were used:

Cytochromegene
- Forward: GTGGCTAGTGGCTACTGTATTG
- Reverse: TCCCAAAGTGCTGGGATTA

IL**-6 (amplicon length: 151 bp)**
- Forward: CCCAGGAGAAGATTCCAAAGAT
- Reverse: GCTGCTTTCACACATGTTACTC

β**-actin (reference gene)**
- Forward: AGTTGCGTTACACCCTTTCTT
- Reverse: CACCTTCACCGTTCCAGTTT

Statistical analysis

All values are reported as mean ± SD obtained from three separate experiments. Statistical evaluation between the groups was carried out through two-way ANOVA, complemented by Tukey's post hoc multiple comparison test.

Results and Discussion

The characteristic properties of the RO-AuNPs viz., spectroscopic, crystalline, surface imaging, and size were retrieved from sophisticated modern equipment and techniques. Further synthesized gold nanoparticles were evaluated for antimicrobial and cytotoxic activity on A549 lung cancer cell line

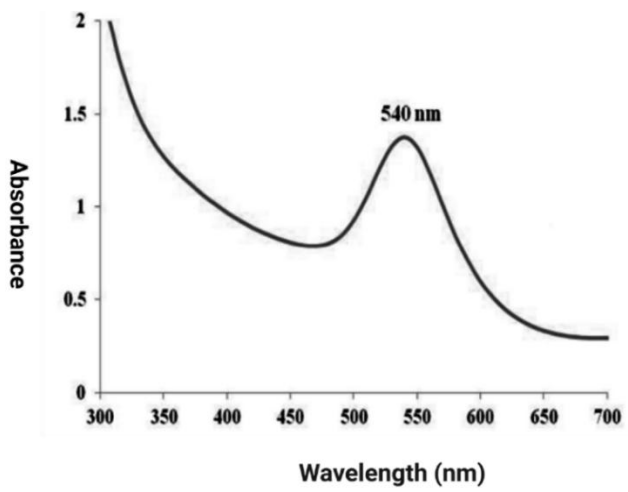

Fig. 3. UV-Vis spectrophotometer graph of RO-AuNPs.

XRD analysis: Characterization of the crystalline structure of the nanoparticles was performed using XRD analysis at room temperature, employing Cu Kα radiation (λ ≈ 1.5406 Å) within a 2θ range of 0°–90°. The diffraction profile, presented in Fig. 4, displayed peaks at 38.5°, 44.64°, 64.82°, 77.63°, and 81.68°, which correspond to the 111, 200, 220, 311, and 222 lattice planes. This analytical data is well agreeable with the fcc crystalline structure by consulting the JCPDS data. Further, the mean crystal size of synthesized NPs was obtained as 42 nm by employing the Debye-Scherer equation: $D = k\lambda/\beta\cos\theta$.

Field emission scanning electron microscopic analysis (FESEM): A Scanning electron microscope focuses electron beams on the surface of the sample and detects the scattered and released electron waves back from the surface to provide

UV-Vis spectroscopy: The initial clue about the synthesis of RO-AuNPs was a transition in the color from pale yellow to ruby red, as shown in (Fig. 2), which prompted us to further analysis. The sample was subjected to UV-Vis spectroscopic analysis and a sharp peak of absorption at 540 nm was recorded as shown in Fig. 3, which is well consistent with standard AuNP absorption peak. Pertinently here, in this case, reduction and subsequent stabilization of Au III ions to Au metal/nanoparticles occur with the help of bioactive molecules present in the plant extract. Plants are complicated biological ensembles of innumerable biomolecules that assist in the reduction, stability, and functionality of nanoparticles during nano synthesis. The fact is that the phytochemicals present in *R. officinalis*, including flavonoids, terpenoids, alkaloids, anthocyanins, phenolic acids, proteins, and vitamins, are reported to be causative agents for bio-reduction and subsequently stabilize the nanoarchitectures. The green synthetic plant-mediated method for the formation of nanomaterials surpasses the chemical methods which involve the use of biologically and environmentally incompatible conventional chemical reducing agents (sodium borohydride, sodium formaldehyde, formamide, p-aminobenzoic acid, p-aminosalicylic acid) and chemical stabilizers like polyvinyl alcohol (PVA), polyethyleneimine (PEI), glycol chitosan (GC) (Sofi *et al*., 2022; Ali *et al*., 2021).

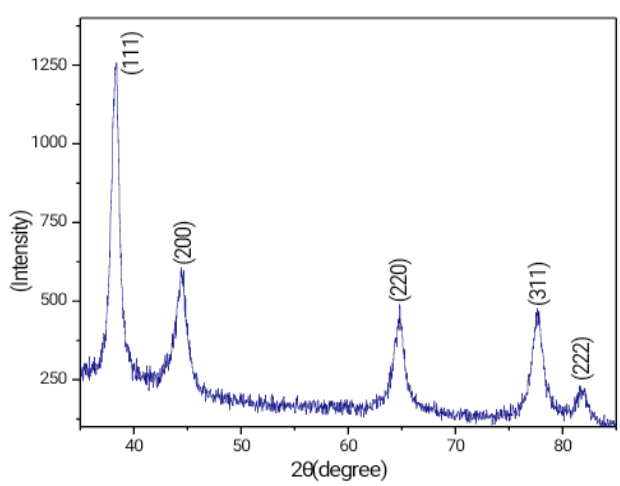

Fig. 4. XRD graph of RO-AuNPs depicting five diffraction peaks.

information about the surface topography and particle diameter. It is high-resolution and a powerful analytical technique. From FESEM analysis, we found AuNPs size in the range of 16-57 nm using ImageJ software and were predominantly spherical (Fig. 5). EDAX analysis further revealed the % elemental composition present in the sample as shown in (Fig. 6). A sharp and strong peak of gold was observed together with the small peaks of other elements (C, O, Al, and Si), indicating the accumulation of gold atoms into nanostructures.

Antimicrobial activity of RO-AuNPs: Plant-mediated production of gold nanoparticles (AuNPs) has gained popularity in recent years owing to their antibacterial capabilities. AuNPs are effective antibacterials because of their unique qualities, like a high surface-to-volume ratio,

tunable size, diversified composition morphologies, and effective interaction or adherence to microbial bio membranes. AuNPs have the ability to change the permeability and membrane potential of microbial cells, which can impair physiological functions and eventually stop growth or cause cell death. These nanoparticles have shown promising results against a variety of pathogenic bacterial and fungal species. AuNPs' antimicrobial effect may also be linked to their interaction with enzymes or coenzymes (such as ATP synthase and NADH), sulphur or phosphorus-containing biomolecules, and ribosomes found in microbial cells. By interfering with these components, AuNPs disrupt essential physiological processes in microbial cells, resulting in their inhibition or death. Given the global rise in antimicrobial resistance, green-synthesized AuNPs derived from plant extracts present a promising alternative for future antimicrobial therapies (Nisar *et al*., 2019; Castillo-Henríquez *et al*., 2020).

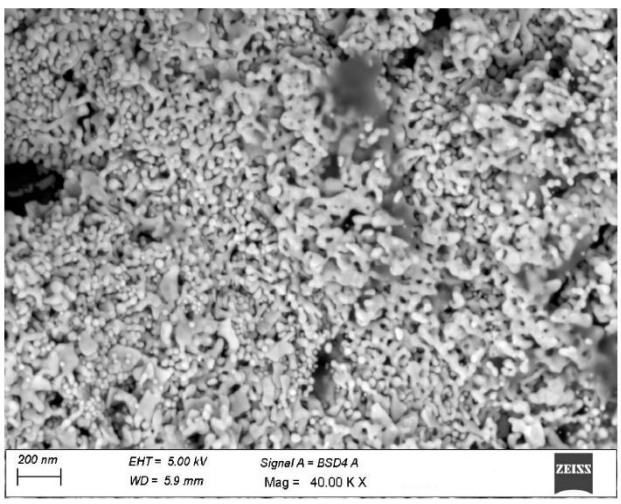

Fig. 5. FESEM micrographs of RO-AuNPs.

Element	Weight %	Atomic %
C K	11.17	58.37
O K	2.26	8.87
AlK	1.43	3.32
SiK	1.21	2.71
AuM	83.92	26.73

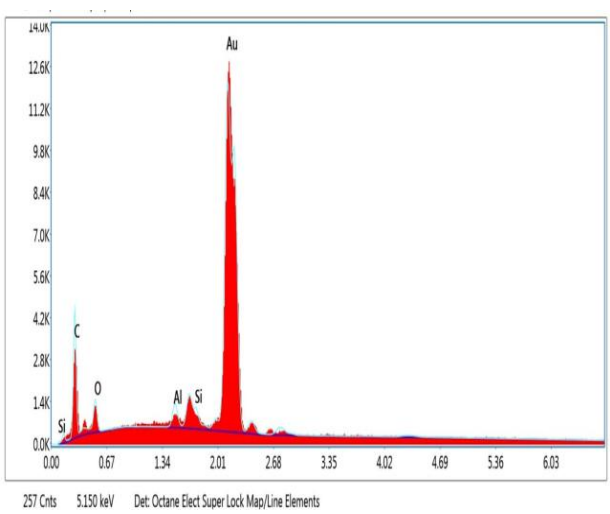

Fig. 6. EDAX graph of RO-AuNPs showing strong Au peak with other small peaks of C, O, Si and Al.

In the present study, the antimicrobial activity of phytomediated synthesized AuNPs from the aqueous *R officinalis* leaf extract was investigated against five microbial species. From the zones of inhibition observed in Figs. 7 and 8, it can be concluded that the synthesized AuNPs demonstrated potent inhibitory activity against *S. aureus, E. faecalis, E. coli,* and *P. aeruginosa*. For *C. albicans*, inhibitory activity was observed at higher nanomaterial concentrations.

Similarly, other studies have reported the antimicrobial potential of biosynthesized AuNPs from different plant extracts. AuNPs synthesized from mulberry leaf extract by (Adavallan & Krishnakumar (2014) demonstrated effective inhibition against *Staphylococcus aureus* (Gram-positive) and *Vibrio cholerae* (Gram-negative) bacteria. Another study, reported that AuNPs synthesized from *Jasminum auriculatum* leaf extract demonstrated antibacterial action against *K. pneumonia, E. coli, S. pyogenes,* and *S. aureus* (Balasubramanian*et al*., 2020). Furthermore, a study using a mixture of *Adiantum capillus* veneris and *Pteris quadriureta* extracts to synthesize AuNPs revealed antifungal activity against *Aspergillus flavus, Aspergillus niger, Aspergillus fumigates Trichophyton rubrum,* and *Scedosporium apiospermum* (Rautray & Rajananthini, 2020).These studies support our results, indicating that gold nanoparticles produced using *R. officinalis* leaf extract have strong antimicrobial effects. Interestingly, the aqueous extract alone failed to show any antimicrobial activity against the pathogens tested. The absence of antimicrobial activity in the crude aqueous extract, in contrast to the pronounced efficacy of RO-AuNPs, suggests that nanoparticle formation plays a decisive role in bioactivity enhancement. Increased surface area, nanoscale dimensions, and improved interaction with microbial membranes likely contribute to this effect. Similar enhancement of antimicrobial properties following nanoparticle synthesis has been reported previously, where plant extracts showed little to no antimicrobial action while the corresponding nanoparticles displayed significant inhibitory zones against pathogenic strains, attributed to their unique physicochemical interactions with microbial cell walls (Adavallan & Krishnakumar (2014); Kalantari & Turner. (2024); Castillo-Henríquez *et al*., 2020).This suggests that the antimicrobial properties observed may be specifically attributed to the green synthesized gold nanoparticles, rather than the plant extract itself.

Cytotoxicity of RO-AuNPs on A549 lung cancer cell line: Gold nanoparticles have several distinguishing characteristics that make them a promising choice for anticancer research. AuNPs(*Rosmarinus officinalis* gold nanoparticles) are known to have a relatively long retention period in the body, which means that they can stay in the target tissue for a longer period of time, allowing for more sustained therapeutic effects. Besides, AuNPs have been found to be biocompatible with cells and tissues, meaning that they are less likely to cause

harmful effects on healthy cells. This is an important consideration when developing new anticancer treatments (Zhuang *et al*., 2025). Green methodologies for nanoparticle synthesis often use plant extracts, representing a sustainable and eco-friendly alternative to chemical approaches. These techniques often use natural chemicals found in plants, which may enhance the bio value of the plant extract and provide further health advantages. The inherent therapeutic qualities of medicinal plant extracts make them valuable for nanoparticle synthesis. The ability of gold nanoparticles (AuNPs) to impede cancer cell proliferation and induce programmed cell death has been well-documented, supporting their relevance in cancer treatments (Chauhan*et al*., 2021; Liu *et al*., 2019; Patil *et al*., 2019; Wu *et al*., 2019).

In this research, RO-AuNPs were found to effectively inhibit A549 lung cancer cells, as evidenced by IC_{50} values of 33.60 µg/mL at 24 hs and 23.12 µg/mL at 48 hs in MTT assays. This underscores their potential as an antilung cancer agent.

Our study demonstrated that the cytotoxicity of RO-AuNPs increased with concentration, indicating a clear dose-dependent anticancer effect (Fig. 9). This trend aligns with findings from previous studies on plant-mediated gold nanoparticles. For example, Patel *et al*., 2019 found that AuNPs derived from *Lonicera japonica* flower extract displayed strong, dose-dependent cytotoxicity in HeLa cervical cancer cells. Likewise, Wu *et al*., 2019 found that, AuNPs produced from *Abies spectabilis* extract exhibited substantial anticancer efficacy in T24 bladder carcinoma, with an IC_{50} of 20 µg/mL. In another relevant study, synthesized AuNPs from licorice root extract, which demonstrated cytotoxic effects against HepG-2 liver cancer cells (IC_{50} = 23 µg/mL) and MCF-7 breast cancer cells (IC_{50} = 50 µg/mL) (Al-Radadi, 2021). However, it is important to conduct a detailed investigation to better understand and develop future therapeutics based on the results of these studies that are in agreement with our study. This will offer a deeper understanding of the underlying mechanisms and factors contributing to the observed outcomes, as well as potential limitations or confounding factors.

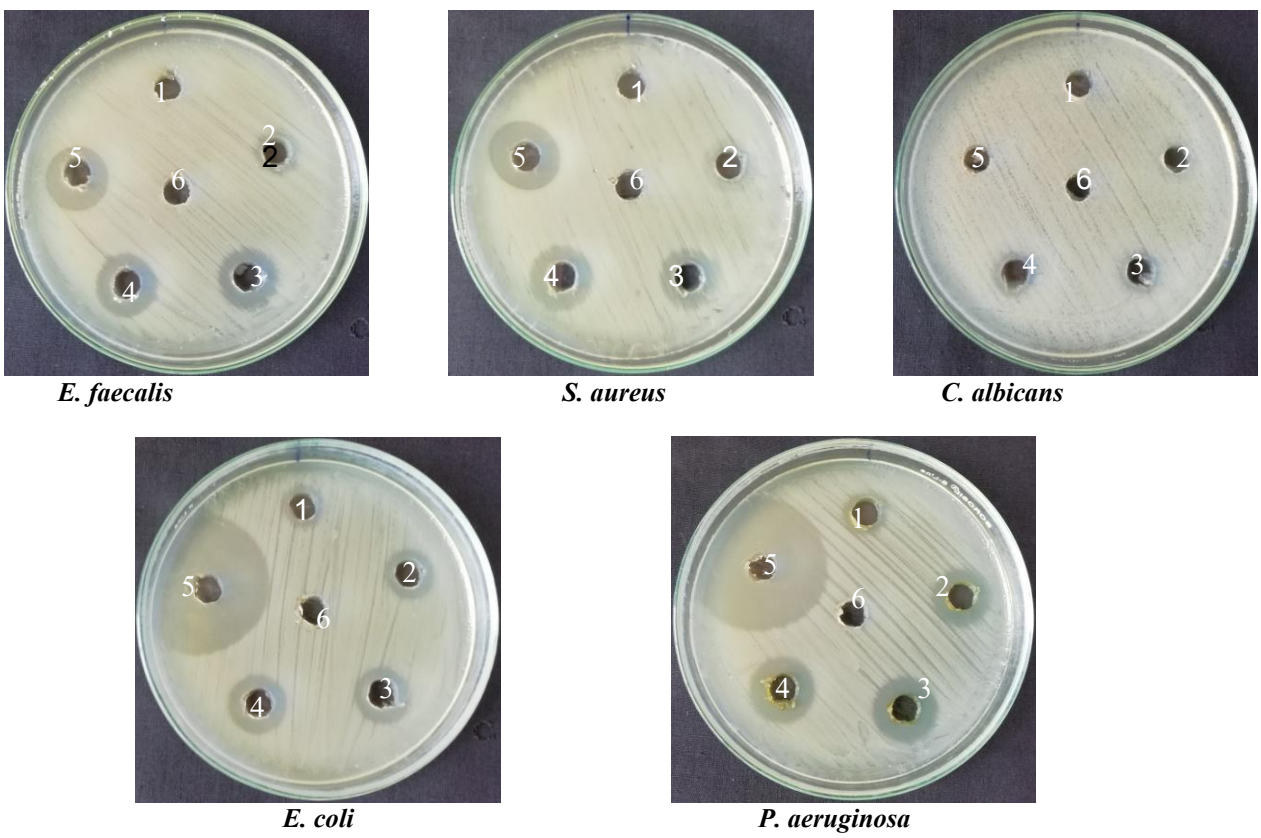

Fig. 7. Demonstrates the antimicrobial efficacy of the **RO-AuNPs** derived from *R*. officinalis through the well diffusion technique. Each Petri dish is labelled with numbers (1-4) corresponding to the wells into which 25, 50, 75 and 100 µL of **RO-AuNPs** were introduced from stock solution 1 mg/mL. (5) for the positive control Ciprofloxacin, Fluconazole and Ampilox, 25 µL (1 mg/mL) were used. 6 well was introduced with negative control DMSO. The antimicrobial activity of RO-AuNPs exhibited a clear concentration-dependent trend across all tested microorganisms. As the volume of nanoparticles increased from 25 to 100 µL, a corresponding increase in the zone of inhibition was observed, indicating a dose-dependent inhibitory effect

Confirmation of apoptosis by AO/PI Staining: To morphologically validate apoptosis, AO/PI dual staining was performed on RO-AuNP-treated A549 cells. This method differentiates live, necrotic and early apoptotic cells by evaluating the extent of membrane damage and chromatin condensation Jaisankar *et al*., 2022). Treated cells exhibited classic apoptotic features, including membrane damage and chromatin condensation as indicated by orange/red fluorescence in PI-positive nuclei. In contrast, untreated control cells retained green fluorescence with intact nuclei, signifying viability Fig. 10.

Pro-apoptotic gene expression (Cytochrome C): To further elucidate the molecular mechanism of apoptosis, we assessed the *Cytochrome C*expression, a pivotal pro-apoptoticgene involved in the mitochondrial pathway. RT-PCR analysis revealed a significant upregulation of *Cytochrome C* mRNA in RO-AuNP-treated A549 cells compared to control Fig.11. Cytochrome C release from mitochondria into the cytosol is a key event that activates downstream caspases, leading to irreversible apoptosis. Our findings suggest that RO-AuNPs initiate the intrinsic apoptotic pathway, likely through mitochondrial membrane depolarization and oxidative stress (Bharadwaj*et al*., 2021; Morsy*et al*., 2025; Wani *et al*., 2023; Ramalingam *et al*., 2016). Mechanistically, the cytosolic release of Cytochrome C promotes the formation of the apoptosome complex through its interaction with apoptotic protease activating factor-1 (Apaf-1) and procaspase-9. This complex facilitates caspase-9 activation, which subsequently triggers executioner caspases such as caspase-3 and caspase-7, culminating in DNA fragmentation and irreversible apoptotic cell death. (Nisha et al., 2024; Baharara et al., 2016). Although caspase activity was not directly measured in the present study, the observed upregulation of Cytochrome C strongly suggests activation of the caspase-dependent intrinsic apoptotic cascade, a mechanism widely reported for green-synthesized gold nanoparticles in lung cancer models

Anti-inflammatory activity via IL-6 downregulation: Chronic inflammation is known to facilitate cancer progression by promoting proliferation, angiogenesis, and immune evasion. Interleukin-6 (IL-6) is a central pro-inflammatory cytokine frequently overexpressed in lung tumors and associated with poor prognosis (Liu *et al*., 2021).Therefore, targeting IL-6 signaling presents a promising therapeutic strategy. In our study, RT-PCR results showed that RO-AuNPs significantly downregulated *IL-6* expression in A549 cells, indicating anti-inflammatory activity Fig. 12. This suppression may be attributed to the synergistic action of gold nanoparticles and phytochemicals present in *R. officinalis*, such as carnosic acid and ursolic acid, which have documented anti-inflammatory properties(Nisha *et al*., 2024). Beyond its inflammatory role, IL-6 is a critical regulator of the tumor microenvironment, where it promotes cancer cell survival, angiogenesis, immune evasion, and resistance to apoptosis primarily through persistent activation of the JAK/STAT3 signaling pathway Kitamura et al., 2017; Fisher et al., 2014) . Suppression of IL-6 expression, as observed in RO-AuNP-treated A549 cells, may therefore disrupt pro-tumorigenic signaling networks within the tumor microenvironment, enhancing susceptibility to apoptosis and reducing inflammatory support for tumor progression . The combined inhibition of IL-6 signaling and induction of mitochondrial apoptosis suggests that RO-AuNPs may exert dual anticancer effects by directly targeting tumor cells while simultaneously modulating inflammation-driven tumor support mechanisms.

Therapeutic relevance and future perspectives: By inducing apoptosis (as evidenced by AO/PI staining and *Cytochrome C* expression) and reducing inflammatory signaling (*IL-6* suppression), RO-AuNPs display a dual mechanism of anticancer action. These properties highlight the therapeutic potential of green-synthesized AuNPs not only for cytotoxicity but also for immune modulation within the tumor microenvironment. Future studies should investigate ROS production, caspase activation, and in vivo antitumor effects to further validate the clinical utility of RO-AuNPs.

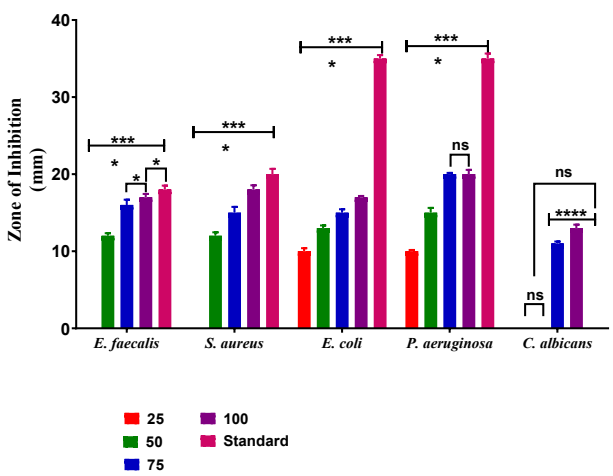

Fig. 8. Antimicrobial activity RO-AuNPs against selected bacterial and fungal strains at various concentrations compared to the standard drug. The antimicrobial activity of RO-AuNPs exhibited a clear concentration-dependent trend across all tested microorganisms. As the volume of nanoparticles increased from 25 to 100 µL, a corresponding increase in the zone of inhibition was observed, indicating a dose-dependent inhibitory effect. Values are shown as mean ± SD. Two-way ANOVA with Tukey's test

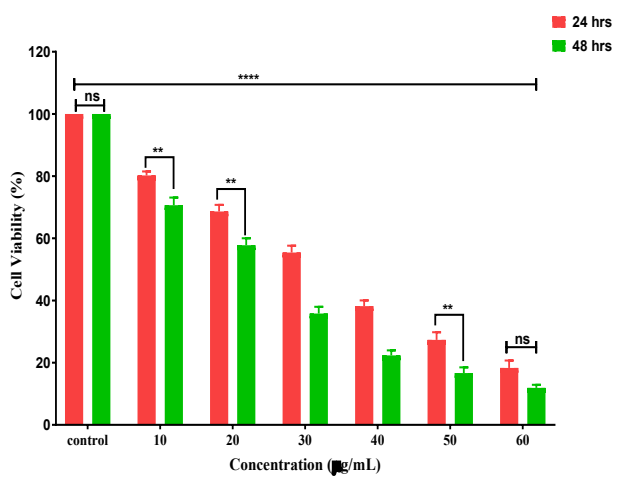

Fig. 9.The cytotoxic effect of RO-AuNPs on A549 cells was evaluated across a concentration gradient. Cytotoxicity analysis revealed a pronounced dose- and time-dependent reduction in A549 cell viability following RO-AuNP treatment. Increasing nanoparticle concentrations resulted in progressive loss of cell viability, with a more pronounced effect observed at 48 h compared to 24 h exposure. Values are shown as mean ± SD. Two-way ANOVA with Tukey's test.

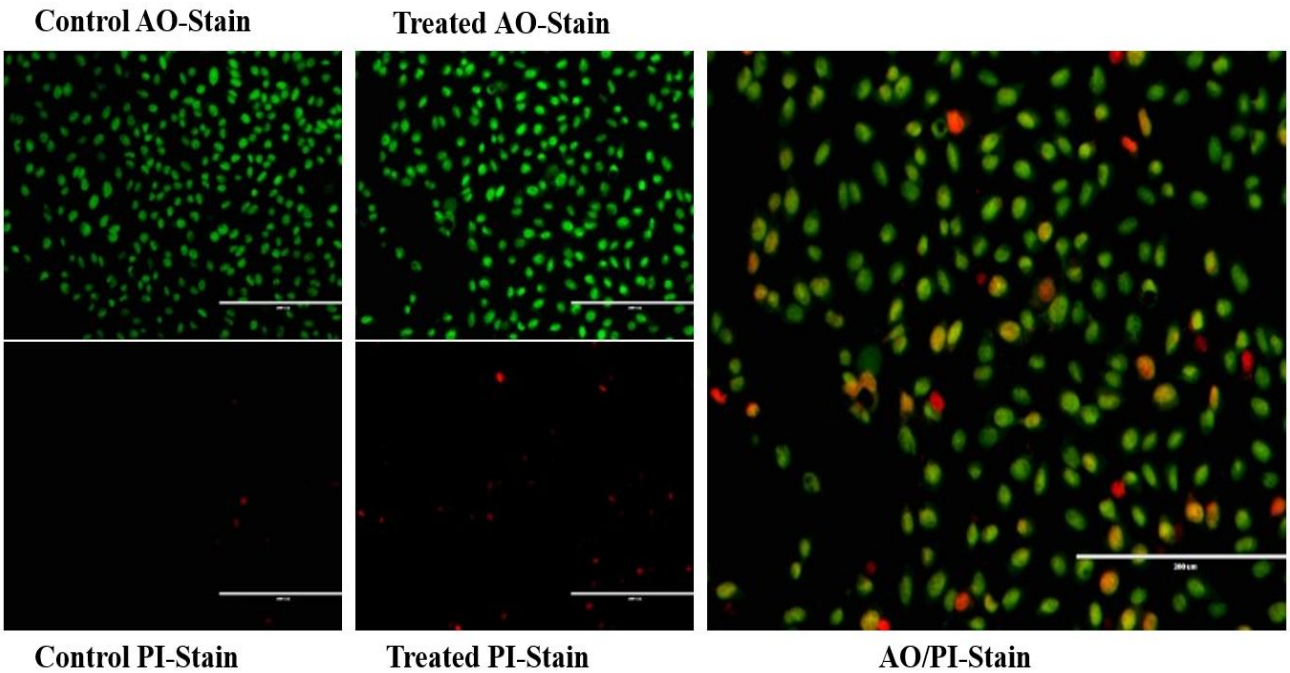

Fig. 10. Fluorescence microscopy images showing apoptosis in A549 lung cancer cells using dual (AO/PI) staining. The predominance of orange/red fluorescence in treated cells indicates compromised membrane integrity and chromatin condensation, confirming apoptosis

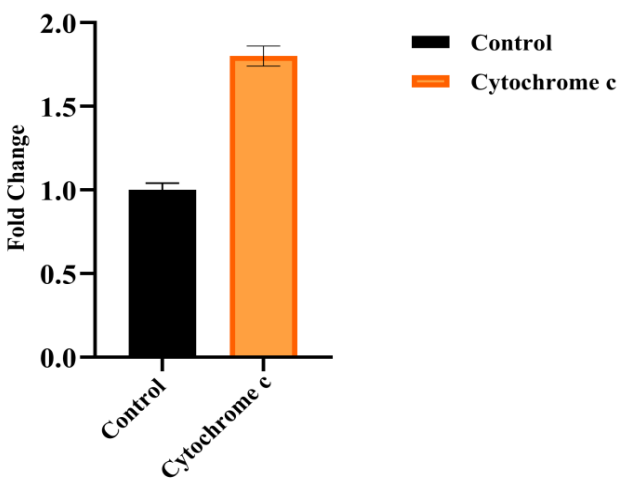

Fig. 11. Graphical representation of mRNA expression analysis of Cytochrome C in RO-AuNPs treated A549 cells. The graph illustrates the significant upregulation of the proapoptotic gene compared to the control (β-actin), with results statistically significant at *p<0.05.

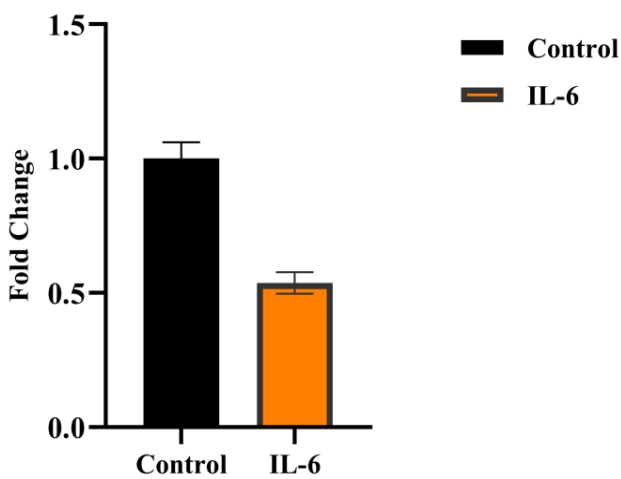

Fig. 12. Graphical representation of mRNA expression analysis of IL-6 in RO-AuNPs A549 treated cells. The graph illustrates the significant downregulation of this gene compared to the control (β-actin), with results statistically significant at *p<0.05.

Conclusion

The development of therapeutic nanomaterials through sustainable and eco-friendly methods is gaining significant attention in drug discovery. The application of green synthesis, particularly with plant extracts and biomaterials, is a promising strategy for creating nanoparticles with unique features and therapeutic uses. Gold nanoparticles produced via *R. officinalis* extract have exhibited notable antimicrobial and anticancer activity. This method not only reduces costs but also minimizes environmental impact, making it a sustainable substitute for conventional chemical synthesis. Gene expression analysis further confirmed significant upregulation of pro-apoptotic cytochrome c and downregulation of pro-inflammatory IL-6 mRNA levels, supporting their dual anticancer and anti-inflammatory potential. These multifunctional properties suggest possible translational applications, such as antimicrobial surface coatings, biomedical device integration, and adjunct therapeutic strategies in cancer treatment.. However, further investigations are essential to elucidate their mechanism of action and validate their clinical safety and efficacy. In particular, comprehensive biosafety assessment, in vivo validation, and evaluation of biodistribution are required before considering clinical application It will also be important to investigate the potential for any negative impacts on the environment or unintended consequences.

Overall, these findings are promising and highlight the potential for plant-incorporated gold nanomaterials to be developed as a new class of therapeutics with broad-spectrum activity against infections and cancer cells.

Conflicts of Interest: The authors state that there is no competing interest

Source of Funding: Sathyabama laboratory facility is being used and no funding was obtained for this research.

Authors contribution A M. T، M.A.S. wrote the original draft, conducted the investigation, proposed the methodology, performed formal analysis, reviewed and edited the manuscript, curated the data, provided resources and software, managed the project, and conceptualized the study. A.N. and B.K.N. contributed to writing the original draft, supervised, validated the study, and reviewed and edited the manuscript**.**

Acknowledgements

The authors express gratitude to Department of Biomedical Engineering, Sathyabama Institute of Science and Technology Chennai, for providing the laboratory facilities.

References

Adavallan, K. and N. Krishnakumar. 2014. Mulberry leaf extract mediated synthesis of gold nanoparticles and its antibacterial activity against human pathogens. *Adv. Nat. Sci. Nanosci. Nanotech.*, 5(2): 025018.

Ali, S., M. Bacha, M.R. Shah, W. Shah, K. Kubra, A. Khan and M. Ali. 2021. Green synthesis of silver and gold nanoparticles using *Crataegusoxyacantha* extract and their urease inhibitory activities. *Biotechnol. Appl. Biochem.*, 68(5): 992-1002.

Al-Radadi, N.S. 2021. Facile one-step green synthesis of gold nanoparticles (AuNp) using licorice root extract: antimicrobial and anticancer study against HepG2 cell line. *Arab. J. Chem.*, 14(2): 102956.

Azharuddin, M., G.H. Zhu, D. Das, E. Ozgur, L. Uzun, A.P. Turner and H.K. Patra. 2019. A repertoire of biomedical applications of noble metal nanoparticles. *Chem. Comm.*, 55(49): 6964-6996.

Baharara, J., T. Ramezani, A. Divsalar, M. Mousavi and A. Seyedarabi. 2016. Induction of apoptosis by green synthesized gold nanoparticles through activation of caspase-3 and -9 in human cervical cancer cells. *Avicenna J. Med. Biotechnol***.**, 8(2): 75.

Balasubramanian, S., S.M.J. Kala and T.L. Pushparaj. 2020. Biogenic synthesis of gold nanoparticles using *Jasminum auriculatum* leaf extract and their catalytic, antimicrobial and anticancer activities. *J. Drug Deliv. Sci. Technol.*, 57: 101620.

Bharadwaj, K.K., B. Rabha, S. Pati, T. Sarkar, B.K. Choudhury, A. Barman and N.H. Mohd Noor. 2021. Green synthesis of gold nanoparticles using plant extracts as beneficial prospect for cancer theranostics. *Molecules*, 26(21): 6389.

Botteon, C.E.A., L.B. Silva, G.V. Ccana-Ccapatinta, T.S. Silva, S.R. Ambrosio and R.C.S. Veneziani. 2021. Biosynthesis and characterization of gold nanoparticles using Brazilian red propolis and evaluation of its antimicrobial and anticancer activities. *Sci. Rep.*, 11(1): 1974.

Castillo-Henríquez, L., K. Alfaro-Aguilar, J. Ugalde-Álvarez, L. Vega-Fernández, G. Montes de Oca-Vásquez and J.R. Vega-Baudrit. 2020. Green synthesis of gold and silver nanoparticles from plant extracts and their possible applications as antimicrobial agents in the agricultural area. *Nanomaterials*, 10(9): 1763.

Chauhan, A., T. Khan and A. Omri. 2021. Design and encapsulation of immunomodulators onto gold nanoparticles in cancer immunotherapy. *Int. J. Mol. Sci.*, 22(15): 8037.

Choi, H.K., M.J. Lee, S.N. Lee, T.H. Kim and B.K. Oh. 2021. Noble metal nanomaterial-based biosensors for electrochemical and optical detection of viruses causing respiratory illnesses. *Front. Chem.*, 9: 672739.

Chomczynski, P. and N. Sacchi. 1987. Single-step method of RNA isolation by acid guanidinium thiocyanate-phenol-chloroform extraction. *Anal. Biochem.*, 162(1): 156-159.

Fisher, D.T., M.M. Appenheimer and S.S. Evans. 2014. The two faces of IL-6 in the tumor microenvironment. Semin. Immunol**.**, 26(1): 38–47.

Gabrielson, J., M. Hart, A. Jarelöv, I. Kühn, D. McKenzie and R. Möllby. 2002. Evaluation of redox indicators and the use of digital scanners and spectrophotometer for quantification of microbial growth in microplates. *J. Microbiol. Methods*, 50(1): 63-73.

Gong, Z., H.T. Chan, Q. Chen and H. Chen. 2021. Application of nanotechnology in analysis and removal of heavy metals in food and water resources. *Nanomaterials*, 11(7): 1792.

Guliani, A., A. Kumari and A. Acharya. 2021. Green synthesis of gold nanoparticles using aqueous leaf extract of *Populus alba*: characterization, antibacterial and dye degradation activity. *Int. J. Environ. Sci. Technol***.**, 18(12): 4007–4018.

Halahlah, A., E. Kavetsou, I. Pitterou, S. Grigorakis, S. Loupassaki, L.A. Tziveleka and A. Detsi. 2021. Synthesis and characterization of inclusion complexes of rosemary essential oil with various β-cyclodextrins and evaluation of their antibacterial activity against *Staphylococcus aureus*. *J. Drug Deliv. Sci. Technol.*, 65: 102660.

Hassanisaadi, M., G.H.S. Bonjar, A. Rahdar, S. Pandey, A. Hosseinipour and R. Abdolshahi. 2021. Environmentally safe biosynthesis of gold nanoparticles using plant water extracts. *Nanomaterials*, 11(8): 2033.

Jaisankar, E., R.S. Azarudeen and M. Thirumarimurugan. 2022. A study on the effect of nanoscale MgO and hydrogen bonding in nanofiber mats for controlled drug release along with *In vitro* breast cancer cell line and antimicrobial studies. *ACS Appl. Bio Mater.*, 5(9): 4327-4341.

Kalantari, H., & Turner, R. J. (2024). Structural and antimicrobial properties of synthesized gold nanoparticles using biological and chemical approaches. *Frontiers in Chemistry*, 12: 1482102.

Kamyshny, A. and S. Magdassi. 2019. Conductive nanomaterials for 2D and 3D printed flexible electronics. *Chem. Soc. Rev.*, 48(6): 1712-1740.

Kitamura, H., Y. Ohno, Y. Toyoshima, J. Ohtake, S. Homma, H. Kawamura and A. Taketomi. 2017. Interleukin-6/STAT3 signaling as a promising target to improve the efficacy of cancer immunotherapy. **Cancer Sci.**, 108(10): 1947–1952.

Levchenko, I., S. Xu, G. Teel, D. Mariotti, M.L.R. Walker and M. Keidar. 2018. Recent progress and perspectives of space electric propulsion systems based on smart nanomaterials. *Nat. Commun.*, 9(1): 879.

Liu, K., Z. He, J.F. Curtin, H.J. Byrne and F. Tian. 2019. A novel, rapid, seedless, *in situ* synthesis method of shape and size controllable gold nanoparticles using phosphates. *Sci. Rep.*, 9(1): 7421.

Liu, Y., Y. Gao and T. Lin. 2021. Expression of interleukin-1 (IL-1), IL-6 and tumor necrosis factor-α (TNF-α) in non-small cell lung cancer and its relationship with the

occurrence and prognosis of cancer pain. *Ann. Palliat. Med.*, 10(12): 127592766-127512766.

Ma, X., Y. Tian, R. Yang, H. Wang, L.W. Allahou, J. Chang and A. Poma. 2024. Nanotechnology in healthcare, and its safety and environmental risks. *J. Nanobiotechnol.*, 22(1): 715.

Morsy, H.M., M.Y. Zaky, N.Y. Yassin and A.Y. Khalifa. 2025. Nanoparticle-based flavonoid therapeutics: pioneering biomedical applications in antioxidants, cancer treatment, cardiovascular health, neuroprotection, and cosmeceuticals. *Int. J. Pharm.*, 670: 125135.

Nisar, P., N. Ali, L. Rahman, M. Ali and Z.K. Shinwari. 2019. Antimicrobial activities of biologically synthesized metal nanoparticles: an insight into the mechanism of action. *J. Biol. Inorg. Chem.*, 24: 929-941.

Nisha, R.S.K. Sachan, A. Singh, A. Karnwal, A. Shidiki and G. Kumar. 2024. Plant-mediated gold nanoparticles in cancer therapy: exploring anti-cancer mechanisms, drug delivery applications and future prospects. *Front. Nanotechnol.*, 6: 1490980.

Nisha, R.S.K. Sachan, A. Singh, A. Karnwal, A. Shidiki and G. Kumar. 2024. Plant-mediated gold nanoparticles in cancer therapy: exploring anti-cancer mechanisms, drug delivery applications and future prospects. *Front. Nanotechnol***.**, 6: 1490980.

Patil, M.P., E. Bayaraa, P. Subedi, L.L.A. Piad, N.H. Tarte and G.D. Kim. 2019. Biogenic synthesis and characterization of gold nanoparticles using *Lonicera japonica* and their anticancer activity on HeLa cells. *J. Drug Deliv. Sci. Technol.*, 51: 83-90.

Patil, T.P., A.A. Vibhute, S.L. Patil, T.D. Dongale and A.P. Tiwari. 2023. Green synthesis of gold nanoparticles via *Capsicum annum* fruit extract: characterization, antiangiogenic, antioxidant and anti-inflammatory activities. *Appl. Surf. Sci. Adv***.**, 13: 100372.

Peng, H., S. Zhang, Q. Chai and Z. Hua. 2024. Green synthesis of gold nanoparticles using *Acorus calamus* leaf extract and study on their anti-Alzheimer potential. *Biotechnol. Bioprocess Eng***.**, 29(1): 157–163.

Rahbardar, M.G. and H. Hosseinzadeh. 2020. Therapeutic effects of rosemary (*Rosmarinus officinalis* L.) and its active constituents on nervous system disorders. *Iran. J. Basic Med. Sci.*, 23(9): 1100.

Ramalingam, V., S. Revathidevi, T. Shanmuganayagam, L. Muthulakshmi and R. Rajaram. 2016. Biogenic gold nanoparticles induce cell cycle arrest through oxidative stress and sensitize mitochondrial membranes in A549 lung cancer cells. *RSC Adv.*, 6(25): 20598-20608.

Rautray, S. and A.U. Rajananthini. 2020. Therapeutic potential of green synthesized gold nanoparticles. *BioPharm. Int.*, 33: 30-38.

Sajid, M. 2022. Nanomaterials: Types, properties, recent advances, and toxicity concerns. *Curr. Opin. Environ. Sci. Health*, 25: 100319.

Salamatullah, A.M., K. Hayat, S. Arzoo, A. Alzahrani, M.A. Ahmed, H.M. Yehia and M.M. Althbiti. 2021. Boiling technique-based food processing effects on the bioactive and antimicrobial properties of basil and rosemary. *Molecules*, 26(23): 7373.

Schaming, D. and H. Remita. 2015. Nanotechnology: from the ancient time to nowadays. *Found. Chem.*, 17: 187-205.

Shang, Y., M. Hasan, G.J. Ahammed, M. Li, H. Yin and J. Zhou. 2019. Applications of nanotechnology in plant growth and crop protection. *Molecules*, 24(14): 2558.

Sharma, P.K., S. Dorlikar, P. Rawat, V. Malik, N. Vats and M. Sharma. 2021. Nanotechnology and its application. *Nanotechnol. Cancer Manag.*, 1-33.

Siddique, S. and J.C. Chow. 2020. Gold nanoparticles for drug delivery and cancer therapy. *Appl. Sci.*, 10(11): 3824.

Singh, P., S. Pandit, V.R.S.S. Mokkapati, A. Garg, V. Ravikumar and I. Mijakovic. 2018. Gold nanoparticles in diagnostics and therapeutics for human cancer. *Int. J. Mol. Sci.*, 19(7): 1979.

Sofi, M.A., A. Nanda, E. Raj and M.A. Sofi. 2022. Phytochemical profiling of the methanolic root extract of *Lavatera cashmeriana* using GC-MS and evaluation of its potential antimicrobial activity. *Res. J. Pharm. Technol.*, 15(12): 5707-5713.

Sofi, M.A., A. Nanda, M.A. Sofi, T. Sheikh and G.A. Rather. 2022. *In vitro* evaluation of antimicrobial and anticancer potential of *Artemisia absinthium* growing in Kashmir Himalayas. *J. Appl. Nat. Sci.*, 14(3).

Sofi, M.A., M.A. Sofi, A. Nanda, B.K. Nayak, Z. Othman and M.Z. Sadikan. 2025. Exploring the therapeutic potential of *Podophyllum hexandrum* root extract: chemical composition, antimicrobial efficacy, and antioxidant and anticancer activities. *Scientifica*, 2025(1): 5100547.

Sofi, M.A., S. Sunitha, M.A. Sofi, S.K. Pasha and D. Choi. 2022. An overview of antimicrobial and anticancer potential of silver nanoparticles. *J. King Saud Univ. Sci.*, 34(2): 101791.

Theyyathel, A.M., M.A. Sofi, A. Nanda, M.A. Sofi and B.K. Nayak. 2025. Exploring the therapeutic potential of *Rosmarinus officinalis*: a review study. *J. Nat. Remedies.*, 25(1): 33-48.

Wani, A.K., N. Akhtar, S.R. Tug M., P.K. Jha, S.K. Mallik, S. Sinha and H.P. Devkota. 2023. Targeting apoptotic pathway of cancer cells with phytochemicals and plant-based nanomaterials. *Biomolecules*, 13: 194.

Wu, T., X. Duan, C. Hu, C. Wu, X. Chen, J. Huang and S. Cui. 2019. Synthesis and characterization of gold nanoparticles from *Abies spectabilis* extract and its anticancer activity on bladder cancer T24 cells. *Artif. Cells Nanomed. Biotechnol.*, 47(1): 512-523.

Yaqoob, A.A., H. Ahmad, T. Parveen, A. Ahmad, M. Oves, I.M. Ismail and M.N. Mohamad Ibrahim. 2020. Recent advances in metal decorated nanomaterials and their various biological applications: a review. *Front. Chem.*, 8: 341.

Zhuang, L., Y. Lian and T. Zhu. 2025. Multifunctional gold nanoparticles: bridging detection, diagnosis, and targeted therapy in cancer. *Mol. Cancer*, 24(1): 228.